Journal of Solid State Chemistry 182 (2009) 3076–3084

Contents lists available at ScienceDirect

Journal of Solid State Chemistry

journal homepage: www.elsevier.com/locate/jssc

Preparation and characterization of mesoporous N-doped and sulfuric acid treated anatase TiO_2 catalysts and their photocatalytic activity under UV and Vis illumination

Robert Kun [a], Sándor Tarján [b], Albert Oszkó [c], Torben Seemann [d], Volker Zöllmer [d], Matthias Busse [d], Imre Dékány [a,b,*]

[a] Supramolecular and Nanostructured Materials Research Group of the Hungarian Academy of Sciences, University of Szeged, Aradi vt. 1, H-6720 Szeged, Hungary
[b] Department of Colloid Chemistry, University of Szeged, Aradi vt. 1, H-6720 Szeged, Hungary
[c] Department of Solid State and Radiochemistry, University of Szeged, Aradi vt. 1, H-6720 Szeged, Hungary
[d] Fraunhofer Institute for Manufacturing Technology and Applied Materials Research, IFAM, Wienerstrasse 12, 28359 Bremen, Germany

ARTICLE INFO

Article history:
Received 9 April 2009
Received in revised form
20 August 2009
Accepted 23 August 2009
Available online 28 August 2009

Keywords:
TiO_2
N-doping
Acid treatment
Phenol
Photocatalysis
Visible light

ABSTRACT

Nitrogen-doped TiO_2 catalysts were prepared by a precipitation method. The samples were calcined at 400 °C for 4 h in air. X-ray diffraction (XRD), X-ray photoelectron spectroscopy (XPS), low temperature N_2-adsorption was used for structural characterization and UV-diffuse reflectance (UV-DR) was applied to investigate the optical properties of the as-prepared samples. It was found that microporous N-doped catalysts have solely anatase crystalline structure. Acidic treatment of the calcined samples was performed using sulfuric acid agitation. The crystalline structure remained unchanged due to surface treatment, while the porosity and the surface areas (a^S_{BET}) were decreased dramatically. Optical characterization of the doped catalysts showed that they could be excited by visible light photons in the 400–500 nm wavelength range ($\lambda_{g,1} = \sim 390$ nm, $\lambda_{g,2} = \sim 510$ nm). It was also established that surface treatment enhances the Vis-light absorption of the N-TiO_2 powders. Finally the catalysts were tested in the photocatalytic degradation of phenol in aqueous suspensions. Two different light sources were used; one of them was a UV-rich high pressure Hg-lamp, while the other was a tubular visible light source. We found that using visible light illumination N-doped, acid treated TiO_2 samples were more catalytically active than non-doped TiO_2 catalysts.

1. Introduction

Titanium dioxide (TiO_2) is a well known photocatalyst material and it can be used in environmental remediation, e.g. air purification or waste water treatment. Some of the first publications related to the TiO_2 mediated photooxidation of organic pollutants in air and aqueous media were published several decades ago [1–5]. TiO_2 has a number of advantageous properties, for instance it is non-toxic, photo- and chemically stable, and relatively inexpensive. Still there are some open questions, e.g. how the efficiency of the photocatalytic processes could be improved and some authors have reported on the low quantum efficiency of the catalysts [6,7] in addition the light scattering of such heterogeneous colloid systems (i.e. suspension) makes the quantum efficiency data evaluation inaccurate and unreliable [8]. However the biggest disadvantage of the TiO_2 particles is that they can be activated only with UV-light ($\lambda < 380$ nm), which comprises only less than 10% of the natural solar spectrum [9]. It would be favorable and more economic if the catalyst particles could be excited with the visible light of the solar spectrum. Many attempts have been made to reduce the relatively wide band gap (E_g=3.2 eV) of anatase TiO_2 particles (band gap narrowing) to shift the absorption edge of the TiO_2 particles toward the visible region. One approach is doping of the titanium dioxide crystal lattice with transition metal ions like Co, Cr, Fe, Mn, Ni, V and W etc. (i.e. cationic doping or metal-ion implantation) [10–13] which resulted in Ti^{4+} ion substitution with the above mentioned cations in order to alter the electronic and optical properties of the original material, but the thermal instability and an increase in the number of the generated charge carrier recombination centers have a limitation on the performance of these doped materials. Another possibility is the non-metal-doping in which the non-metal species (O^{2-}) of the TiO_2 lattice is replaced with other ions or "vacancies" i.e. reduced TiO_x samples are prepared [14]. It is more difficult to replace the O^{2-} anion with other anions due to differences in charge states and ionic radii. A variety of non-metal elements, such as S, C, P, B, N [15–21] have been used as dopants for TiO_2. Visible-light responsive

* Corresponding author at: Supramolecular and Nanostructured Materials Research Group of the Hungarian Academy of Sciences, University of Szeged, Aradi vt. 1, H-6720 Szeged, Hungary. Fax: +36 62 544042.
E-mail address: i.dekany@chem.u-szeged.hu (I. Dékány).

0022-4596/$ - see front matter © 2009 Elsevier Inc. All rights reserved.
doi:10.1016/j.jssc.2009.08.022

photocatalyst materials have been successfully prepared by N-doping. Authors reported on the increased photocatalytic activity due to the successful band gap narrowing by the N-implantation into the TiO_2 crystals [22–26]. Based on theoretical band structure calculations or XPS studies, researchers try to explain the origin of the visible-light response of the N-TiO_2 samples. Recently the most general opinion about the increased visible-light response of the nitrogen-doped TiO_2 is the band gap narrowing by mixing of the O 2*p* states with the N 2*p* states [27]. Nakamura et al. reported that the increased light sensitivity is due to an N-induced mid-gap level, which was generated slightly above the top of the O 2*p* valence band [28]. Another suggestion from Ihara et al. is that oxygen-deficient sites (below the conduction band) generated on the grain-boundaries in the TiO_2 polycrystalline structure are responsible for the visible-light response and the nitrogen dopants are important as reoxidation blockers [29]. N-doped TiO_2 photocatalysts can be prepared by different ways. Some of the methods use organic N-sources such as amines [30] or urea, while others use inorganic source like ammonia gas or its aqueous solution [31–34]. As well as the high temperature ammonia gas treatment of the pure solid TiO_2 and wet chemical methods, such as the co-precipitation, other doping techniques can also be found in the literature. For example Kobayakawa et al. reported the preparation of N-TiO_2 by means of the co-annealing of precipitated $Ti(OH)_4$ powders with urea [35]. Recently, researchers have tried to combine the different doping procedures with the surface modification to improve the photocatalytic efficiency due to synergistic effects. Highly active photocatalysts can be prepared by impregnation of the amorphous metal oxide precipitates followed by a high temperature calcination step [36]. The idea for this is that the visible-light response can be enhanced if the number and strength of the acidic surface sites on the TiO_2 particles are increased by means of PO_4^{3-} or SO_4^{2-} ion impregnation. In this manner usually acids, like H_3PO_4 or H_2SO_4 are used as impregnators [37].

In the present study we report on the preparation, characterization and the visible-light driven photocatalysis of N-doped TiO_2 samples prepared by means of co-precipitation combined with sulfate ion impregnation technique. The samples were characterized by XRD, XPS and N_2-adsorption measurements and the optical properties were analyzed by UV–Vis diffuse reflectance spectroscopy. The samples were tested in the photodegradation of phenol as model pollutant in aqueous suspensions. Two different light sources (UV-rich and visible) were applied to demonstrate the increased visible-light response of our catalysts. The photodegradation curves were derived from HPLC analyses.

2. Experimental

2.1. Materials

N-doped TiO_2 catalysts were prepared from titanium tetraisopropoxide $Ti(iOPr)_4$ (Fluka Chemika, puriss) as organic precursor. For the doping procedure urea (Fluka Chemika, puriss) was used and sulfuric acid (0.5 M, H_2SO_4, Reanal, Hungary) was applied by the acid treatment of the catalysts. Sodium hydroxide (NaOH, Reanal, Hungary, pro anal.) was used in the surface acidity titration experiments. The reaction medium was purified (ion exchanged) water. In the photocatalytic activity studies phenol (Aldrich, 99+) was used as model substance.

2.2. Methods

The XRD experiments were carried out in a Philips X-ray diffractometer (PW 1930 generator, PW 1820 goniometer) with CuKα radiation (λ=0.15418 nm) at ambient temperature in the 20–60° (2Θ) range applying 0.02° (2Θ) step size. The average crystalline sizes (D) were obtained by means of the Scherrer equation [$D=k\lambda/(\beta\cos\Theta)$, where β is the line broadening ($\beta=\beta_s-\beta_0$, where β_s and β_0 are the half-widths of the XRD peak of the sample and of the silicon standard), k is related to the crystallite shape, and λ and Θ are the radiation wavelength and Bragg angle, respectively] from the (101) Bragg reflection of anatase found at 25.5° (2Θ).

Specific surface areas of the N-doped TiO_2 samples were determined by a Micromeritics gas sorption analyzer (Gemini Type 2375) at 77 K in liquid nitrogen. The adsorption and desorption branches of the isotherms were determined. Prior to measurements the samples were pretreated in vacuum (ca. 0.01 torr) at 393 K for 2 h. The sample holder was loaded with ca. 0.1–0.3λ_g sample. The adsorption isotherms were analyzed by means of the BET equation, the micropore volume data were determined with the de Boer's *t-method* [38] and the pore size distribution curves were analyzed by the Barret–Joyner–Halenda (BJH) method [39].

XP spectra were acquired with a SPECS instrument equipped with a PHOIBOS 150 MCD 9 hemispherical electron energy analyzer operated in the FAT mode. The excitation source was the K_α radiation of a magnesium anode ($h\nu$=1253.6 eV). The X-ray gun was operated at 180 W (12 kV, 15 mA). The pass energy was set to 20 eV, the step size was 25 meV, and the collection time in one channel was 150 ms. Typically five scans were combined to produce a single spectrum. The C 1*s* binding energy of adventitious carbon was used as energy reference. It was taken to be 285.1 eV. For data acquisition both manufacturer's (SpecsLab2) and commercial (CasaXPS, Origin) software were used. Before the data analysis X-ray satellites originating from the non-monochromatic excitation source were removed from the spectra.

For the optical characterization of the samples UV-diffuse reflectance apparatus was used. A Micropack HPX-2000 High Power Xenon Lamp served as light source and a Micropack NanoCalc 2000 Spectrometer was applied as detector. Prior to analyses the solid samples were grounded in an agate mortar and the reflection spectra of the same amount of powder samples were recorded using a Micropack ISP-50-8-R-GT integration sphere.

Surface acidity was determined by titration method to prove the increased surface acidity due to sulfuric acid treatment of the calcined catalysts. A given amount of solid sample was dispersed by ultrasonication in boiled off deionized water and analytical NaOH solution was added stepwise into the suspension under a N_2 atmosphere (i.e. avoid CO_2 uptake) while pH was registered precisely. Plotting $f(V_{NaOH})$=pH curves and from the position of inflection point surface acidity per weight unit of catalyst (i.e. the alkali consumption of the catalysts in mmol OH^-/g catalyst unit) can be determined. The photocatalytic disappearance of the phenol and the other generated intermediates in the irradiated suspension was followed by high performance liquid chromatography (HPLC). After the established irradiation time the samples were filtered through 0.22 μm hydrophilic PTFE membranes (Millipore Millex). A Knauer injector, an RP C_{18} column (LiChroCART 125-4, Merck, 125 mm × 4 mm, 5 μm packing), a high-pressure pump (Knauer WellChrom K-1001 pumps) with a supplementary Knauer Degasser, a Knauer WellChrom K-1500 Solvent organizer and UV–Vis detector (Knauer WellChrom UV-detector K-2600) were used. Acetonitrile/water mixture (20/80) was used as eluent.

2.3. Catalyst preparation

2.3.1. Preparation of the N-TiO_2 samples

A simple precipitation method was used to prepare N-doped TiO_2 samples. The calculated amount of urea was dissolved in

200 ml of ion exchanged water. The solution was stirred continuously for 30 min, until the total amount of the urea was dissolved. 20.3 ml of titanium isopropoxide was added dropwise to this solution under vigorous stirring (in the case of the non-doped TiO_2 the precursor was added into ion exchanged water; sample notation: TiO_2, *precip.*, *calcined*). Due to the spontaneous hydrolysis of the titanium dioxide precursor a milky white dispersion was obtained, which was stirred for another hour. The solid precipitate was filtered, and then dried at 30 °C. The dried samples were ground and afterwards calcined at 400 °C for 4 h in a furnace (10 °C/min ramp rate was applied) in air. Due to the high temperature treatment from pale-yellow to vivid-yellow N-doped TiO_2 powders were obtained depending on urea loading. The procedure described above relates to the 1:1=N:Ti sample, but further samples with 3:1 and 5:1=N:Ti molar ratios were also prepared. The notation of the N-doped samples is N-TiO_2.

2.3.2. *Acidic treatment of the* N-TiO_2 *samples*

SO_4^{2-} ion impregnated samples were prepared as follows: $1\lambda_g$ of the solid sample (prepared as described in Section 2.3.1.) was placed into a glass flask and then the appropriate amount of 0.5 M H_2SO_4 solution was added into the vessel. The acidic suspension was stirred for 1 h, followed by the filtration of the solid part and the drying at 30 °C. The notation of these samples is TiO_2-*sulf* and N-TiO_2-*sulf*, where "-*sulf*" refers to the sulfuric acid treatment.

2.4. *Photocatalytic activity studies*

The photocatalytic experiments were carried out in a batch type reactor equipped with immersion type lamp and inner Pyrex-filter to eliminate wavelengths <310 nm. Two different light sources were used in the experiments. A high-pressure Hg-arc lamp (P=150 W, λ_{em}=240–580 nm) was used as UV-rich light source, while a LightTech tubular Vis-rich-lamp (P=15 W, λ_{em}=400–630 nm, λ_{max}=620 nm) was used as visible light source. Constant O_2 flow (60 ml/min) and constant temperature was applied (T=298 K) during each irradiation. Prior to irradiation 375 ml of the suspension, containing the model pollutant (phenol, c_{init}=0.5 mmol/l) and the catalyst material ($c_{catalyst}$=100 mg/100 ml) was introduced into the reactor. The adsorption equilibrium was established after 30 min in dark conditions afterwards the irradiation was started. At given time intervals during the illumination 2 ml portions of the suspension were taken out and further analyzed. The accuracy of the photodegradation studies was found to be $\pm 5\%$ which was determined by three parallel photodegradation experiments in some cases.

3. Results and discussion

3.1. *Structural and optical characterization of the samples*

N-doped TiO_2 (i.e. N-TiO_2 and N-TiO_2-*sulf*) samples were characterized by X-ray diffraction to analyze the crystalline phase and the primary crystalline size of the as-prepared samples. It is known from the literature that the doping has phase stabilizing effect on the anatase crystalline phase upon heat treatment [40,41]. In Fig. 1a the X-ray diffractograms of the N-TiO_2 samples calcined at 400 °C for 4 h are presented. The diffraction peaks marked with letter "*A*" on the figure corresponds to the anatase phase. It is clearly seen that peaks found at 25.5, 38.1, 48.2, and 54.2, 55.3 2Θ degree the (101), (004), (200) and the (105), (211) Bragg reflections were assigned, respectively and the rutile phase was not evident neither in the synthesis nor in the calcination process [42]. The X-ray diffraction patterns of the calcined

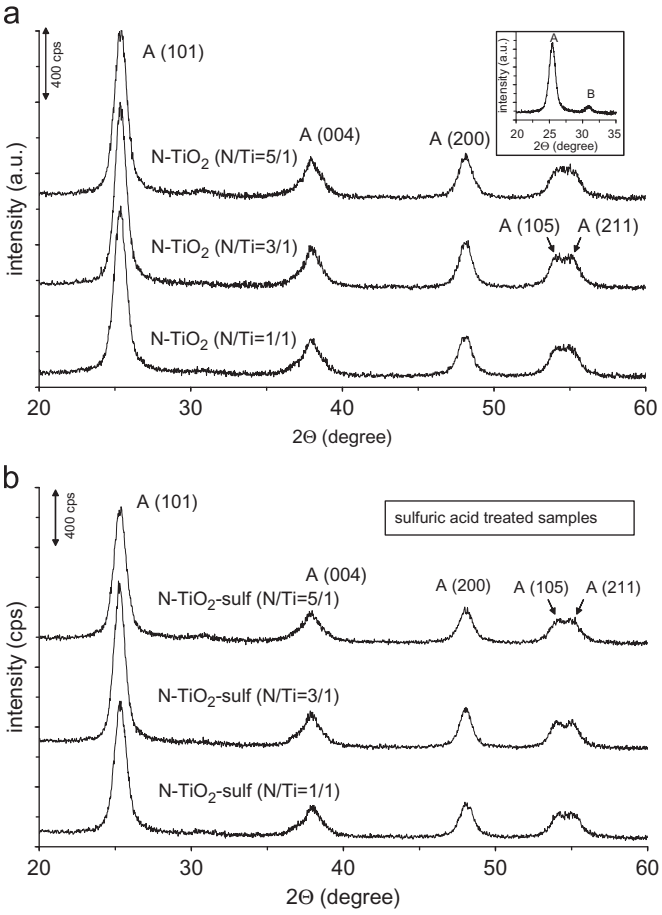

Fig. 1. (a) X-ray diffraction (*A*=anatase, *B*=brookite) patterns of the N-TiO_2 samples prepared with different N/Ti ratio. (b) X-ray diffraction (*A*=anatase) patterns of the sulfuric acid treated N-TiO_2 catalysts prepared with different N/Ti ratio.

(400 °C/4 h) N-TiO_2-sulf samples show similarity with the N-TiO_2 series (see Fig. 1b). It was demonstrated that the crystalline structure of the catalysts and furthermore their bulk composition did not change due to acid treatment. It should be noted, that the non-doped, calcined TiO_2 samples (SO_4^{2-}-treated and non-treated) exhibit brookite phase also (at 30.8 2Θ degree) which polymorph did not form in the N-doped samples (note that a weak brookite reflection can be assigned alone by N/Ti=5/1 sample), see insert in Fig. 1a. The average crystalline sizes in the powder samples were calculated by the Scherrer equation from the anatase (101) reflection found at 25.5° (2Θ). It was found that the average crystalline sizes of the N-TiO_2 samples (d_{mean}=9.7 nm) are slightly lower than that of N-TiO_2-sulf samples (d_{mean}=11 nm). However the lowest crystalline sizes were determined in the case of the non-doped TiO_2 (d_{ave}=8.5 nm). Despite the high N-content in the powder samples Ti_xN_y phase (see JCPDS cards 40-0958, 87-0633, 39-1015, 73-0959) could not be detected in the diffractograms.

While the XRD method generates bulk information, X-ray photoelectron spectra of nitrogen doped TiO_2 samples provided information on the composition of the surface layer. The thickness of this layer is generally regarded as a few nanometers. The high resolution XP spectra showed only one peak with a maximum at about 400 eV for all three untreated samples. According to literature data this signal can be attributed to the N–N bond of adsorbed γ-N_2. The recorded spectra and their deconvolutions are presented in Fig. 2a.

The N 1*s* binding energy only slightly changed with the composition: it was measured 399.95 eV for the 1:1 sample,

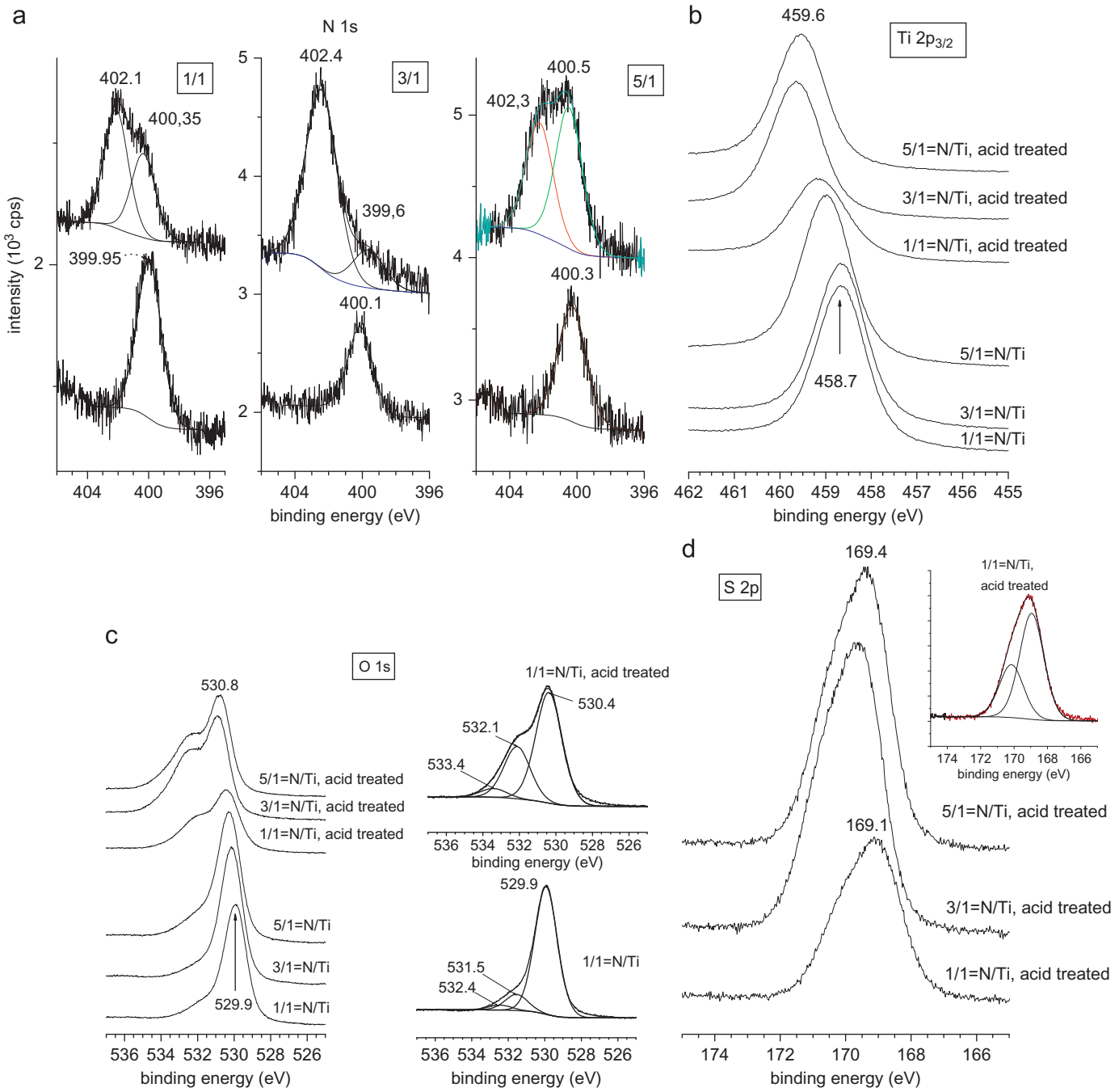

Fig. 2. (a) High resolution (N 1*s*) XP spectra of the N-doped TiO_2 (see N-TiO_2) and sulfuric acid treated N-doped TiO_2 (see N-TiO_2-sulf) series. (b) Ti $2p_{3/2}$ XP spectra of the N-doped-, and sulfuric acid treated N-doped TiO_2 series. (c) O 1*s* XP spectra and deconvolutions of the N-doped-, and sulfuric acid treated N-doped TiO_2 series. (d) S 2*p* XP spectra and deconvolution of the sulfuric acid treated N-doped TiO_2 series.

400.1 eV for the 3:1 and 400.3 eV for the 5:1 one. The surface treatment of the samples led to the appearance of another component in the higher binding energy side of the N 1*s* spectrum envelope. The binding energy of this component was measured 402.1–402.4 eV for all compositions. Taking into account that the error of the energy measurement is at least ± 0.1 eV, these values are practically identical. The origin of this feature is still debated in the literature. Asahi et al. stated that this feature is due to nitrogen weakly physisorbed on the surface [43]. Fang and co-workers somewhat modified this idea saying that both the 400 and 402 eV peaks are from γ-N_2 molecularly chemisorbed to the surface [44]. On the other hand Qiu states [45] that the peaks arising from γ-N_2 appear at 400 and 405 eV. Another explanation is given by Sathish et al. who attribute the feature between 401 and 402 eV to some kind of oxidized nitrogen, possibly to NO or NO_2 [46]. Most authors agree that the appearance of N 1*s* features—including those with binding energy below 400 eV—strongly depends on the nature of the starting materials and the methods by which N doped TiO_2 was produced. From the quantification of the spectra increased nitrogen content can be determined in the case of the acid treated samples (see Table 1). We may suppose that the amount nitrogen due to acid treatment did not change considerably. From this it can be concluded that nitrogen is dispersed in a smaller volume with smaller area

compared to the non-acid treated samples (see textural characterization below). Since the information depth of XPS is also unaltered, one can detect an increased abundance of nitrogen.

Ti 2*p*, O 1*s* and S 2*p* high resolution spectra were also investigated. The Ti $2p_{3/2}$ binding energy was 458.7 eV which corresponds to Ti^{4+}. After the treatment with sulfuric acid the Ti $2p_{3/2}$ binding energy was shifted upwards since adsorbed sulfate species are forming bidentate bridge structures and these could strongly abstract electrons from the neighboring Ti^{4+} cations [47]. In Fig. 2b Ti $2p_{3/2}$ spectra of the two series (i.e. N-TiO_2 and N-TiO_2-*sulf*) are shown and a strong shift from 458.7 to 459.6 eV (i.e. Ti $2p_{3/2}$) upon acid treatment can be observed indicating a strong interaction between sulfate anions and Ti^{4+} cations. On the other hand the possible formation of Ti–O–N bonds also cannot be precluded (see slight shift in binding energy in the case of the non-treated samples in Fig. 2b). The O 1*s* spectra could be deconvoluted into several components see in Fig. 2c. The most intense peak located around 530 eV corresponds to the lattice oxygen in TiO_2. A slight increase of this binding energy could be observed after surface treatment. Two further components could be identified on the O 1*s* spectra. The more intense peak with 531–532 eV binding energy can be attributed to O–H and Ti–O–N bonds while the one between 532.5–533.5 eV may be due to different C–O bonds originating from adventitious carbon. The S $2p_{3/2}$ peak maximum was located at 168.9–169.4 eV, while S $2p_{1/2}$ was located at 170 eV (see Fig. 2d) corresponding to the binding energy generally reported for SO_4^{2-} ions.

Table 1
Quantification of the surface composition of the N-doped TiO_2.

Sample	Atomic percentage				
	Nitrogen	Sulfur	Oxygen	Titanium	Carbon
1:1 N:Ti	0.55–0.78	–	60.9	22.8–26.7	11.7–14.5
3:1 N:Ti			63.8		
5:1 N:Ti			64.9		
1:1 N:Ti acid treated	1.55–1.81	7.31–8.47	64.7–68.5	17.3–18.7	7.05
3:1 N:Ti acid treated					4.09
5:1 N:Ti acid treated					8.81

Table 2
BET surface area and porosity values for the calcined, N-doped TiO_2 samples.

Sample	a_{BET}^{S} (m^2/g)[a]	d_{pore} (nm)[b]	v_{mp} (ncm^3/g)[c]
N-TiO_2 (N/Ti=1/1)	111	3.36	1.68×10^{-3}
N-TiO_2 (N/Ti=3/1)	109	3.76	1.02×10^{-3}
N-TiO_2 (N/Ti=5/1)	116	3.75	1.70×10^{-3}
N-TiO_2-sulf (N/Ti=1/1)	66	3.76	–
N-TiO_2-sulf (N/Ti=3/1)	53	4.92	–
N-TiO_2-sulf (N/Ti=5/1)	68	4.86	–
TiO_2, precip., calcined	132	4.87	1.71×10^{-3}
TiO_2-sulf, precip., calc.	101	4.83	–

[a] Specific surface area data obtained from the BET-model.
[b] Mean pore diameter derived from the maximum values of the BJH pore size distribution curves.
[c] Micropore volume data in normal cm^3/g, calculated by deBoer's *t*-plot method.

From the N_2-adsorption measurements two important parameters, namely the surface area and the porosity can be determined. Both parameters are crucial from the point of view of the catalysis, because often higher surface area results in increased catalytic activity. In our case adsorption and desorption isotherms were also recorded and the BET-method was used to calculate the surface areas of the catalysts. In Table 2 the calculated values are summarized. In Fig. 3a some of the adsorption isotherms of the samples are presented. All of the isotherms are type *IV*, with the typical hysteresis loops in the 0.5–0.7 p/p_0 range. Reaching p_r=1 value the adsorption isotherms are bending toward the ordinate axis which indicates the high extent of outer surfaces in the samples. Interestingly, the isotherms of the samples before and after the surface treatment show similarity but increasing N/Ti ratio in the samples the hysteresis loop became narrower assuming narrower pore size

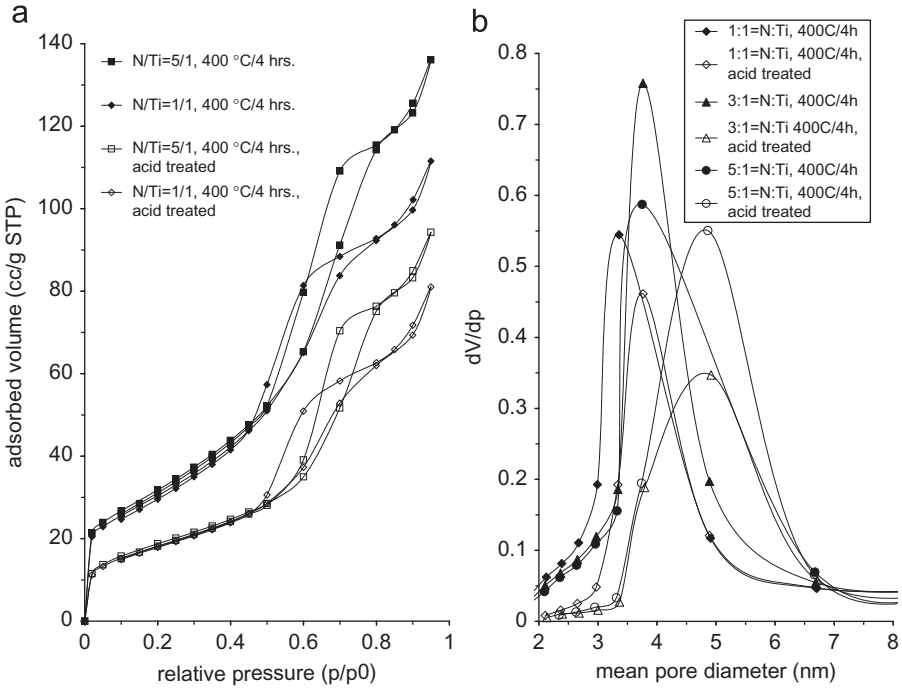

Fig. 3. (a) Low temperature N_2-adsorption isotherm of the N-doped TiO_2 (N-TiO_2) and sulfuric acid treated N-doped TiO_2 (N-TiO_2-sulf) samples. (b) BJH pore size distribution curves of the calcined N-doped TiO_2 catalysts.

distribution in the samples. In the same time the maximum adsorbed volume values are dropped by about 50% due to the sulfuric acid treatment indicating decreased surface area. From Table 2 it can be seen that the determined BET surface area is more or less the double prior to surface treatment and the non-treated samples have microporous structure. As the surface area of the samples decreased due to acid treatment in parallel they also lost microporous character, which was established from the determined micropore volume data using the deBoer's *t-plot* method [48]. The results of the BJH pore size statistics, i.e. the pore size distribution curves are shown in Fig. 3b, which was derived from the desorption branches of the isotherms. From the maximum value of the distribution curves it was revealed that the determined mean pore diameters are smaller in the case of the non-treated samples as it was mentioned before these samples contain more micropores than the acid-treated samples, the values are also represented in Table 2. The same tendency can be observed in the case of the non-doped, calcined titanium dioxide sample (see TiO_2) and the non-doped, calcined and surface treated TiO_2 sample (see TiO_2-sulf). Presumably, due to acid treatment the pore structure of the N-TiO_2-sulf samples did not collapse (i.e. the acid treated samples also have *type IV* isotherms) but the accessibility of the pores with smaller diameter is hindered because of the adsorbed sulfate-species in the micropores (i.e. decreased a^S_{BET} values). So thus, the accessibility of the inner surfaces of the catalyst is blocked.

It is important to know how the catalyst materials are responding to the incident (UV or Vis) light. In other words what is the light absorption threshold (λ_g) which is able to excite the catalyst particles. In Fig. 4 some of the light absorption spectra of the N-doped TiO_2 samples and, of the non-doped, calcined TiO_2 sample are shown. It can be seen that non-doped, calcined TiO_2 has only one light absorption edge (around λ=410 nm) which can be assigned to the band gap of TiO_2. Compared to the non-doped, calcined TiO_2 sample the light absorption of the N-doped samples are much higher in the 400–500 nm wavelength range therefore absorb higher fraction of photons from the visible region. It also can be seen that N-doped samples have two characteristic light absorption edges (see Fig. 4) [49]. One of them corresponds to the band gap of TiO_2 ($\lambda_{g,1}$ = ~390 nm) while other originates from the N-induced midgap level ($\lambda_{g,2}$ = ~510 nm). From the light absorption spectra of the samples the absorption threshold (λ_g) can be determined using the onset of the absorption edges by the section of the fitting lines on the upward and outward section of the spectrum (see insert in Fig. 4) [42,46,50]. The determined λ_g (nm) and the derived band gap energy values are summarized in Table 3, where E_g was calculated using the E_g=1240/λ_g equation. The absorption threshold of the samples in the 300–400 nm wavelength region changes in a narrow range (i.e. within 10 nm). Within one series (acid treated-, and the non-treated sample group) the changes of the $\lambda_{g,1}$ or $E_{g,1}$ of the samples is hardly detectable. Comparing the N-TiO_2 to the N-TiO_2-sulf series it can be established that N-TiO_2 series with smaller average crystalline size (see XRD results) had higher $E_{g,1}$ values than N-TiO_2-sulf (size effect) and the difference was more pronounced with increasing N/Ti ratio (see values in Table 3). The color of the N-doped samples changed from pale yellow to vivid yellow with increasing N/Ti ratio, resulting in enhanced visible light absorption capability in the λ=400–550 nm wavelength range (see Fig. 4) on one hand; and on the other hand the absorption threshold is shifting toward higher wavelength and parallel to that band gap energy is decreasing slightly (see Table 3). As shown in Fig. 5 the SO_4^{2-} ion impregnation has a positive effect on the visible light absorption of the N-doped TiO_2 sample (see insert). It can be seen that light absorbance (in the λ=400–500 nm range) is increasing and the absorption threshold shifted toward higher wavelength upon surface treatment. So thus, sulfuric acid treatment increases the visible light sensitivity of the N-doped TiO_2.

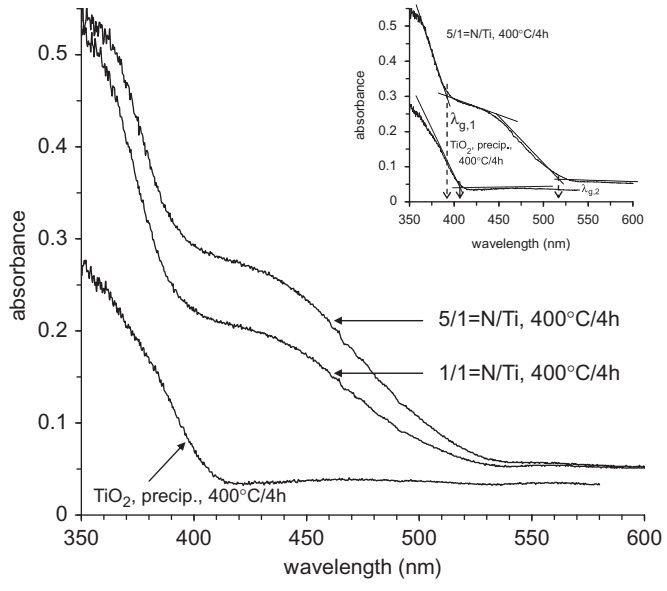

Fig. 4. UV–Vis diffuse reflectance spectra of the calcined N-TiO_2 and the non-doped TiO_2 (insert: determination of the light absorption threshold (i.e. $\lambda_{g,1}$, $\lambda_{g,2}$) by graphical extrapolation).

Table 3
Optical properties of the N-doped TiO_2 samples.

Sample	$\lambda_{g,1}$ (nm)[a]	$E_{g,1}$ (eV)[b]	$\lambda_{g,2}$ (nm)	$E_{g,2}$ (eV)
N-TiO_2 (N/Ti=1/1)	389	3.19	508	2.44
N-TiO_2 (N/Ti=3/1)	390	3.18	512	2.42
N-TiO_2 (N/Ti=5/1)	391	3.17	515	2.41
N-TiO_2-sulf (N/Ti=1/1)	390	3.18	512	2.42
N-TiO_2-sulf (N/Ti=3/1)	393	3.15	517	2.40
N-TiO_2-sulf (N/Ti=5/1)	398	3.11	519	2.39
TiO_2, precip., calcined	407	3.05	–	–

[a] λ_g values were determined using the onset of the light absorption edges.
[b] E_g values were calculated from E_g=1240/λ_g relationship.

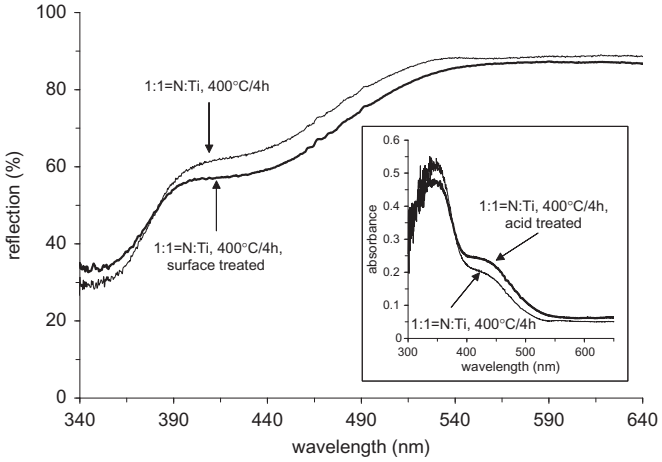

Fig. 5. The effect of the sulfuric acid treatment on the increased Vis-light absorption of the samples determined by UV–Vis diffuse reflectance.

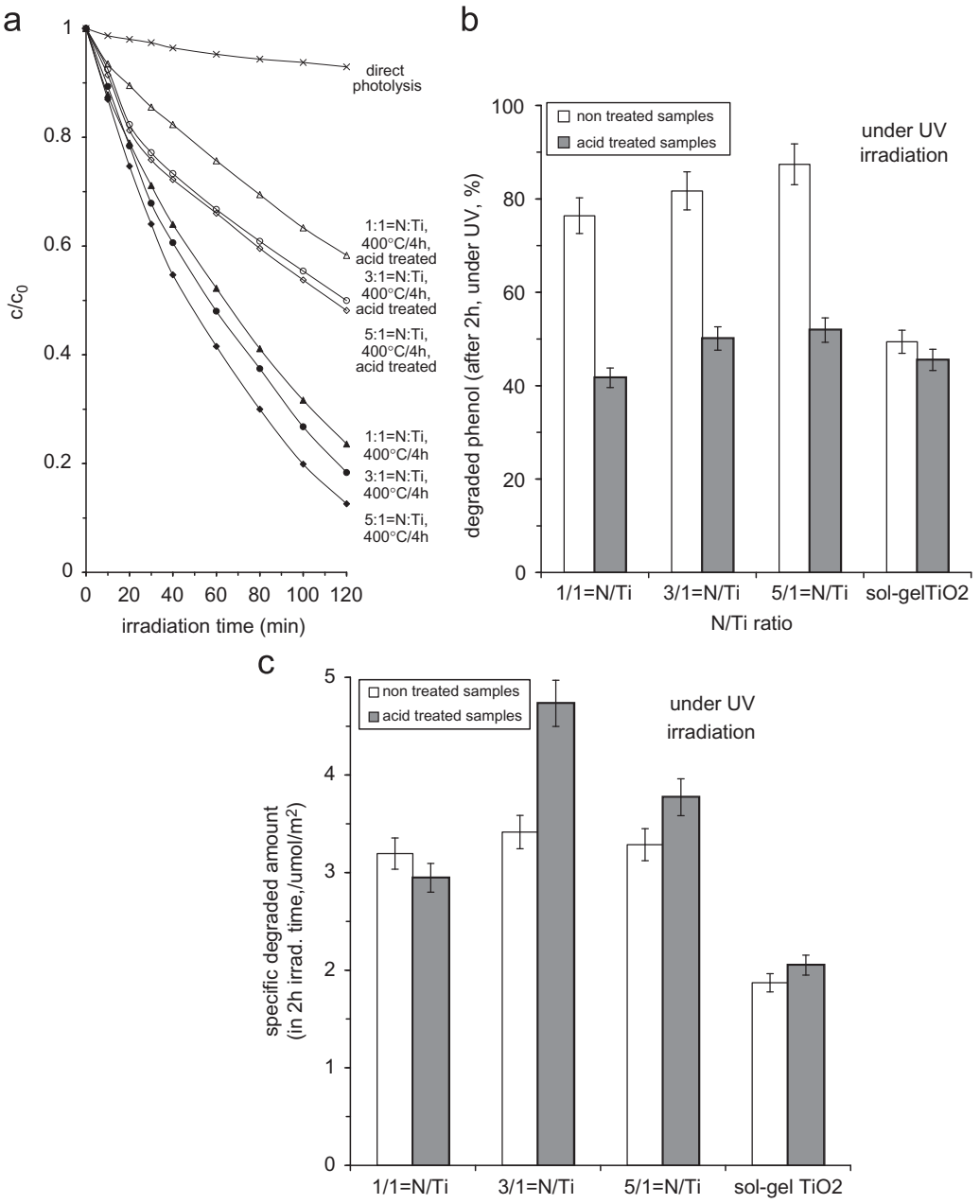

Fig. 6. (a) Phenol degradation curves under UV-rich illumination using different N-doped TiO_2 catalysts. (b) Degraded phenol content in % after 2 h irradiation with UV-rich lamp (P_{lamp}=150 W, λ=240–580 nm). (c) Calculated specific degraded phenol amounts produced by different samples using UV-rich lamp (P_{lamp}=150 W, λ=240–580 nm).

Table 4
Photocatalytic efficiency data on the phenol degradation using different catalysts.

Sample	Residual phenol % after 2 h irradiation time[a]		Specific degraded amount (μmol/m^2)[b]	
	UV (P=150 W, λ=240–580 nm)	Vis (P=15 W, λ_{max}=620 nm)	UV (P=150 W, λ=240–580 nm)	Vis (P=15 W, λ_{max}=620 nm)
N-TiO_2 (N/Ti=1/1)	23.6	83.3	3.19	0.75
N-TiO_2 (N/Ti=3/1)	18.3	85.1	3.42	0.67
N-TiO_2 (N/Ti=5/1)	12.6	76.1	3.29	1.01
N-TiO_2-sulf (N/Ti=1/1)	58.3	82.9	2.95	1.29
N-TiO_2-sulf (N/Ti=3/1)	49.9	81.6	4.73	1.72
N-TiO_2-sulf (N/Ti=5/1)	48.1	74.3	3.77	1.86
TiO_2, precip., calcined	50.6	85.7	1.87	0.53
TiO_2-sulf, precip., calc.	54.5	88.5	2.05	0.55
Direct photolysis	92.9	96.3	–	–

[a] Based on non specified, i.e. original photocatalytic degradation data.
[b] The amount of degraded phenol in μmol after 2 h irradiation time on surface unit of catalysts.

3.2. Photocatalytic activity studies

The catalysts were tested in photodegradation of phenol. The photocatalytic degradation curves using UV-rich source (P=150 W, λ=240–580 nm) are shown in Fig. 6a. The residual phenol content after 2 h irradiation time is summarized in Table 4. Using the N-TiO_2 samples the catalytic efficiency is higher compared to the N-TiO_2-sulf samples. Due to increased N/Ti molar ratio the samples show increased photocatalytic efficiency (see Table 4) in both series. As mentioned previously acid treatment had a negative effect on the porosity and on the extent of the surface area (i.e. it decreases it). This could be the reason for the apparent decreased photocatalytic efficiency in the case of the N-TiO_2-sulf samples. As the catalytically active surface and the porosity are decreasing the apparent efficiency of the catalysis is decreasing, as well. The effect of the direct photolysis (without catalyst) is also represented in this figure. In Fig. 6b the degraded phenol % by the N-doped samples is compared to the amount produced by the non-doped calcined TiO_2 (in addition the photocatalytic efficiencies of the acid treated samples are also shown). In the case of the non-doped, calcined TiO_2 the acid treatment has also negative effect on the photocatalytic activity in this sense. Nevertheless, for lack of visible light sensitivity, latter sample (i.e. non-doped TiO_2) shows decreased catalytic activity. However a different picture can be drawn when not the apparent catalytic data (see Fig. 6a and b) but the specified (normalized) photocatalytic degradation data will be derived and plotted. In Fig. 6c the calculated specific degradation amounts of phenol are presented, where the degraded amount of phenol after 2 h irradiation time were normalized to surface area unit of the catalysts (i.e. μmol/m^2). From the presented results it can be deduced that despite surface area loss and pore characteristics changing upon acid treatment the catalysts exhibited considerable photocatalytic activity thus sulfuric acid treatment had positive effect on the catalytic efficiency (due to increased light absorbance capability of the samples due to acid treatment, see Fig. 5). The calculated normalized data are also presented in Table 4. Furthermore, and as it was mentioned previously adsorbed SO_4^{2-} species can increase the surface acidity [51,52] due to formation of Brønsted acid centers hereby enhance catalytic activity. Accordingly, from the results of the surface acidity measurements it was found that non-treated N-TiO_2 samples had about 0.05–0.06 mmol/g surface acidity while acid treated ones showed at least one order of magnitude higher surface acidity (i.e. 0.5–0.9 mmol/g). Finally the generated surface sulfur complex is strongly able to electron cleavage from basic or electron rich molecules [53], so thus enhance the rate of the photocatalysis.

The obtained catalytic data under visible light illumination (P=15 W, λ_{em}=400–630 nm, λ_{max}=620 nm) are presented in Fig. 7a and b and Table 4. It was found that increasing the N/Ti ratio in the catalysts the amount of the degraded phenol after 2 h irradiation time was increasing, as well. Contrary to the previous photocatalytic experiments (i.e. under UV irradiation) the apparent photocatalytic activity of the acid treated N-doped TiO_2 samples was slightly higher than non-treated samples (note that non-doped TiO_2 showed similar behavior, namely decreased catalytic activity upon acid treatment). Supposedly, the reason for that phenomenon is the increased Vis absorption capability of the acid treated samples which was evidenced only in the case of the N-doped forms (see Fig. 5). However catalytic activity enhancement upon acid treatment is more prominent if surface area normalized catalytic data are discussed, as it can be seen in Fig. 7b. From the presented specific degraded amounts it can be concluded again that acid treatment had positive effect on the catalytic activity which can attribute to enhanced visible light absorption capability, decreased band gap energies and increased surface acidity.

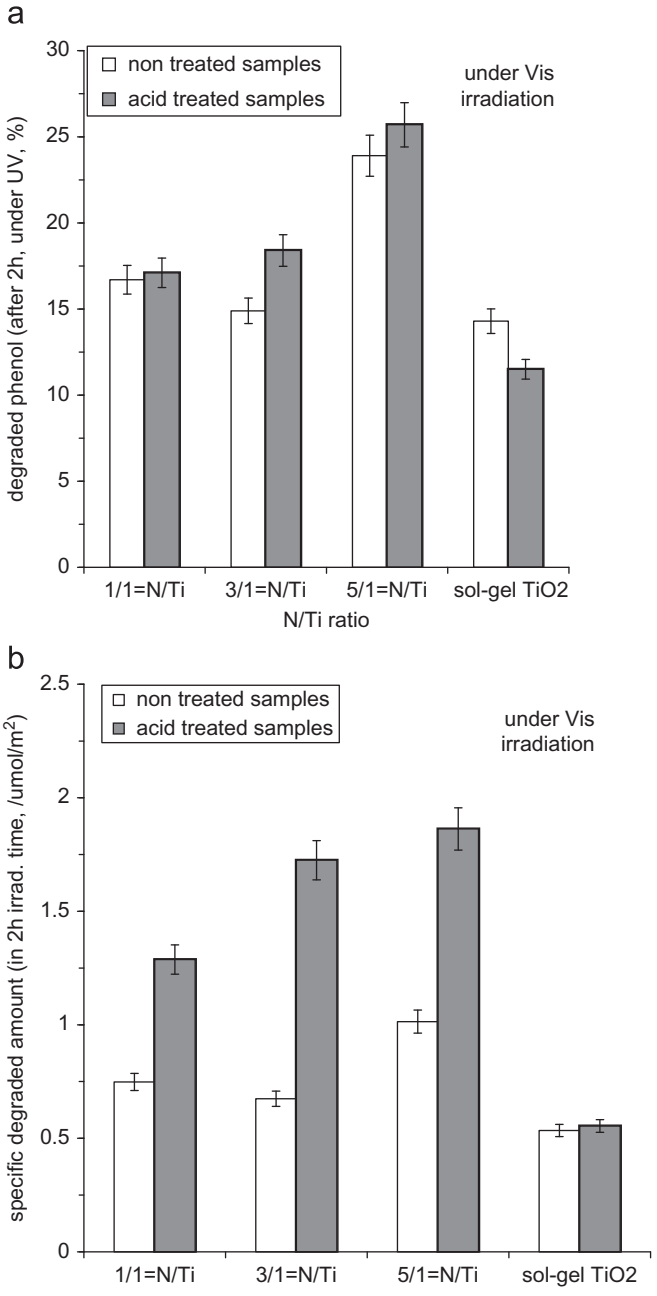

Fig. 7. (a) Degraded phenol content in % after 2 h irradiation with Vis-lamp (P_{lamp}=15 W, λ_{max}=620 nm, λ=400–630 nm). (b) Calculated specific degraded phenol amounts produced by different samples using Vis-lamp (P_{lamp}=15 W, λ_{max}=620 nm, λ=400–630 nm).

4. Conclusion

In the present study the UV and visible light driven photocatalysis of N-doped TiO_2 particles was studied. The common precipitation method was used for the catalyst preparation. Organic titania precursor and urea was used by the syntheses and different N/Ti molar ratios were applied. The as-prepared catalysts were calcined and further treated with sulfuric acid. The calcined samples are in the form of anatase and are microporous. Due to sulfuric acid treatment the catalysts become mesoporous

and the determined specific surface area dropped by 50%, from about 110 to 60 m^2/g. The XP spectra of the samples showed the presence of the adsorbed γ-N_2 and SO_4^{2-}species on the surface. The N-doping of the samples brought about band gap changes (i.e. $\lambda_{g,1}=\sim 390$ nm, $\lambda_{g,2}=\sim 510$ nm) and increased visible light absorption capability of the powders. Using UV-rich source ($P_{lamp}=150$ W) in the photocatalytic experiments the non-treated N-TiO_2 samples showed increased activity, i.e. almost 90% of phenol was degraded in 2 h. The normalized photodegradation data showed that acid treatment could enhance catalytic activity. The N-doping of the TiO_2 samples had positive effect on the visible light driven photocatalysis ($P_{lamp}=15$ W) as well, and it could be further improved by SO_4^{2-} ion impregnation. Accordingly, morphological (crystalline size, porosity, texture, etc.) just as optical-, and surface properties are jointly responsible for the observed photocatalytic activity of the prepared catalysts.

Acknowledgments

The authors wish to thank the financial support of the Hungarian Scientific Fund (OTKA) K73307 and the Fraunhofer Institute for Manufacturing Technology and Applied Materials Research, Fraunhofer-IFAM, Bremen, Germany

Appendix A. Supplementary material

Supplementary data associated with this article can be found in the online version at doi:10.1016/j.jssc.2009.08.022.

References

[1] J.M. Herrmann, J. Disdier, M.N. Mozzanega, P. Pichat, J. Catal. 60 (1979) 369–377.
[2] I. Ilisz, A. Dombi, K. Mogyorósi, A. Farkas, I. Dékány, Appl. Catal. B 39 (2002) 247–256.
[3] M. Muneer, H.K. Singh, D. Bahnemann, Chemosphere 49 (2002) 193–203.
[4] P. Calza, E. Pelizzetti, K. Mogyorósi, R. Kun, I. Dékány, Appl. Catal. B 72 (2007) 314–321.
[5] K. Mogyorósi, A. Farkas, I. Dékány, I. Ilisz, A. Dombi, Environ. Sci. Technol. 36 (2002) 3618–3624.
[6] C.J.G. Cornu, A.J. Colussi, M.R. Hoffmann, J. Phys. Chem. B 105 (2001) 1351–1354.
[7] G. Palmisano, S. Yurdakal, V. Augugliaro, V. Loddo, L. Palmisano, Adv. Synth. Catal. 349 (2007) 964–970.
[8] N. Serpone, A. Salinaro, A. Emeline, V. Ryabchuk, J. Photochem. Photobiol. A 130 (2000) 83–94.
[9] A.L. Linsebigler, G. Lu, J.T. Yates Jr., Chem. Rev. 95 (1995) 735–758.
[10] A. Di Paola, S. Ikeda, G. Marci, B. Ohtani, L. Palmisano, Int. J. Photoenergy 3 (2001) 171–176.
[11] M. Anpo, M. Takeuchi, Int. J. Photoenergy 3 (2001) 89–94.
[12] E. Borgarello, J. Kiwi, M. Grätzel, E. Pelizzetti, M. Visca, J. Am. Chem. Soc. 104 (1982) 2996–3002.
[13] J. Wang, S. Uma, K.J. Klabunde, Appl. Catal. B 48 (2004) 151–154.
[14] I. Nakamura, N. Negishi, S. Kutsuna, T. Ihara, S. Sugihara, K. Takeuchi, J. Mol. Catal. A 161 (2000) 205–212.
[15] M. Shen, Z. Wu, H. Huang, Y. Du, Z. Zou, P. Yang, Mater. Lett. 60 (2006) 693–697.
[16] K.M. Reddy, B. Baruwati, M. Jayalakshmi, M.M. Rao, S.V. Manorama, J. Solid State Chem. 178 (2005) 3352–3358.
[17] K. Takeshita, A. Yamakata, T. Ishibashi, H. Onishi, K. Nishijima, T. Ohno, J. Photochem. Photobiol. A 177 (2006) 269–275.
[18] M. Bettinelli, V. Dallacasa, D. Falcomer, P. Fornasiero, V. Gombacc, T. Montini, L. Romano, A. Speghini, J. Hazard. Mater. 146 (2007) 529–534.
[19] H.F. Yu, J. Phys. Chem. Sol. 68 (2007) 600–607.
[20] T. Umebayashi, T. Yamaki, H. Itoh, K. Asai, Appl. Phys. Lett. 81 (2002) 454–456.
[21] T. Ohno, M. Akiyoshi, T. Umebayashi, K. Asai, T. Mitsui, M. Matsumura, Appl. Catal. A 265 (2004) 115–121.
[22] Y. Wang, C. Feng, Z. Jin, J. Zhang, J. Yang, S. Zhang, J. Mol. Catal. A 260 (2006) 1–3.
[23] T. Tachikawa, Y. Takai, S. Tojo, M. Fujitsuka, H. Irie, K. Hashimoto, T. Majima, J. Phys. Chem. B 110 (2006) 13158–13165.
[24] B. Wawrzyniak, A.W. Morawski, B. Tryba, Int. J. Photoenergy 2006 (2006) 1–8.
[25] M. Sathish, B. Viswanathan, R.P. Viswanath, C.S. Gopinath, Chem. Mater. 17 (2005) 6349–6353.
[26] C. Belver, R. Bellod, S.J. Stewart, F.G. Requejo, M. Fernandez-Garcia, Appl. Catal. B 65 (2006) 309–314.
[27] R. Asahi, T. Morikawa, T. Ohwaki, K. Aoki, Y. Taga, Science 293 (2001) 269–271.
[28] R. Nakamura, T. Tanaka, Y. Nakato, J. Phys. Chem. B 108 (2004) 10617–10620.
[29] T. Ihara, M. Miyoshi, Y. Iriyama, O. Matsumoto, S. Sugihara, Appl. Catal. B 42 (2003) 403–409.
[30] C. Belver, R. Bellod, A. Fuerte, M. Fernandez-Garcia, Appl. Catal. B 65 (2006) 301–308.
[31] S. Yin, K. Ihara, Y. Aita, M. Komatsu, T. Sato, J. Photochem. Photobiol. A 179 (2006) 105–114.
[32] Z. Wang, W. Cai, X. Hong, X. Zhao, F. Xu, C. Cai, Appl. Catal. B 57 (2005) 223–321.
[33] B. Kosowska, S. Mozia, A.W. Morawski, B. Grzmil, M. Janus, K. Kalucki, Solar Energy Mater. Solar Cells 88 (2005) 269–280.
[34] R. Silveyra, L. De La Torre Saenz, W.A. Flores, V.C. Martinez, A.A. Elguezabal, Catal. Today 107–108 (2005) 602–605.
[35] K. Kobayakawa, Y. Murakami, Y. Sato, J. Photochem. Photobiol. A 170 (2005) 177–179.
[36] S.S. Srinivasan, J. Wade, E.K. Stefanakos, Y. Goswami, J. Alloys Compd. 424 (2006) 322–326.
[37] Z.C. Wang, H.F. Shui, J. Mol. Catal. A 263 (2007) 20–25.
[38] J.H. de Boer, B.G. Linsen, T.J. Osinga, J. Catal. 4 (1965) 643–648.
[39] E.P. Barret, L.G. Joyner, P.P. Halenda, J. Am. Chem. Soc. 73 (1951) 373–380.
[40] Y. Zhao, X. Qiu, C. Burda, Chem. Mater. 20 (2008) 2629–2636.
[41] K. Yamada, H. Yamane, S. Matsushima, H. Nakamura, K. Ohira, M. Kouya, K. Kumada, Thin Solid Films 516 (2008) 7482–7487.
[42] C. Liu, X. Tang, C. Mo, Z. Quiang, J. Solid State Chem. 181 (2008) 913–919.
[43] R. Asahi, T. Morikawa, Chem. Phys. 339 (2007) 57–63.
[44] X. Fang, Z. Zhang, Q. Chen, H. Ji, X. Gao, J. Solid State Chem. 180 (2007) 1325–1332.
[45] X. Qiu, C. Burda, Chem. Phys. 339 (2007) 1–10.
[46] M. Sathish, B. Viswanathan, R.P. Viswanath, Appl. Catal. B 74 (2007) 307–312.
[47] X. Wang, J.C. Yu, P. Liu, X. Wang, W. Su, X. Fu, J. Photochem. Photobiol. A 179 (2006) 339–347.
[48] J.H. de Boer, B.C. Lippens, B.G. Linsen, J.C.P. Broekhoff, A. van den Heuvel, T.J. Osinga, J. Coll. Interf. Sci. 21 (1966) 405–414.
[49] J.S. Jang, H.G. Kim, S.M. Ji, S.W. Bae, J.H. Jung, B.H. Shon, J.S. Lee, J. Solid State Chem. 179 (2006) 1067–1075.
[50] R. Kun, M. Szekeres, I. Dékány, Appl. Catal. B Environ. 68 (2006) 49–58.
[51] O. Saur, M. Bensitel, A.B.M. Saad, J.C. Lavalley, C.P. Tripp, B.A. Morrow, J. Catal. 99 (1986) 104–110.
[52] G. Colon, J.M. Sanchez-Espana, M.C. Hidalgo, J.A. Navio, J. Photochem. Photobiol. A 179 (2006) 20–27.
[53] T. Jin, T. Yamaguchi, K. Tanabe, J. Phys. Chem. 90 (1986) 4794–4796.